Single-Channel Recordings from Cultured Human Retinal Pigment Epithelial Cells

JAMES A. FOX, BRUCE A. PFEFFER, and GORDON L. FAIN

From the Jules Stein Eye Institute, University of California at Los Angeles School of Medicine, Los Angeles, California 90024

ABSTRACT We have applied patch-clamp techniques to on-cell and excised-membrane patches from human retinal pigment epithelial cells in tissue culture. Single-channel currents from at least four ion channel types were observed: three or more potassium-selective channels with single-channel slope conductances near 100, 45, and 25 pS as measured in on-cell patches with physiological saline in the pipette, and a relatively nonselective channel with subconductance states, which has a main-state conductance of ~300 pS at physiological ion concentrations. The permeability ratios, P_K/P_{Na}, measured in excised patches were 21 for the 100-pS channels, 3 for the 25-pS channels, and 0.8 for the 300-pS nonselective channel. The 45-pS channels appeared to be of at least two types, with P_K/P_{Na}'s of ~41 for one type and 3 for the other. The potassium-selective channels were spontaneously active at all potentials examined. The average open time for these channels ranged from a few milliseconds to many tens of milliseconds. No consistent trend relating potassium-selective channel kinetics to membrane potential was apparent, which suggests that channel activity was not regulated by the membrane potential. In contrast to the potassium-selective channels, the activity of the nonselective channel *was* voltage dependent: the open probability of this channel declined to low values at large positive or negative membrane potentials and was maximal near zero. Single-channel conductances observed at several symmetrical KCl concentrations have been fitted with Michaelis-Menten curves in order to estimate maximum channel conductances and ion-binding constants for the different channel types. The channels we have recorded are probably responsible for the previously observed potassium permeability of the retinal pigment epithelium apical membrane.

INTRODUCTION

Patch-clamp techniques have been applied primarily to excitable cells, providing information about the unitary events underlying excitation. Although epithelial cell plasma membranes are not, in general, electrically excitable, they do contain

Address reprint requests to Dr. James A. Fox, Dept. of Physiology, S-762, University of California, San Francisco, CA 94143. Dr. Pfeffer's present address is National Eye Institute, National Institutes of Health, Bldg. 9, Rm. 1E-104, Bethesda, MD 20892.

J. GEN. PHYSIOL. © The Rockefeller University Press · 0022-1295/88/02/0193/30$2.00

Volume 91 February 1988 193–222

a variety of conductances that play an essential role in ion and water transport (van Driessche and Zeiske, 1985). Considerable information has been obtained about the properties of these conductances using flux measurements (see, e.g., Lasansky and De Fisch, 1966; Miller and Steinberg, 1982), microelectrode recording techniques (e.g., Miller and Steinberg, 1977; Garcia-Diaz et al., 1983), and noise measurements (Benos, 1983; Lindemann, 1984). However, a detailed understanding of the properties of epithelial cell channels has become possible only with the advent of patch-clamp recording methods (Hamill et al., 1981). Recent patch-clamp studies have shown that some channels in epithelial cells closely resemble those previously described in excitable cells, e.g., calcium-activated potassium channels (Petersen and Maruyama, 1984) and large anion channels (Nelson et al., 1984; Hanrahan et al., 1985; Kolb et al., 1985; Schneider et al., 1985; Krouse et al., 1986). In addition, many channel types not previously seen in nerve and muscle have recently been observed (van Driessche and Zeiske, 1985), particularly in ocular epithelia (Rae and Levis, 1984*b*; Rae, 1985).

We have used patch-clamp methods to investigate the electrophysiological properties of human retinal pigment epithelial cells in culture. The retinal pigment epithelium (RPE) is a transporting epithelium that plays an important role in the local regulation of ions and metabolites in the interphotoreceptor space, that is, the space that separates the apical RPE membrane from the rod outer segments (Steinberg and Miller, 1979; Steinberg et al., 1985). The basal membrane of the RPE is near the blood-vessel–rich choroid, and the processes of the RPE apical membrane surround the rod outer segments. The apical membrane of the RPE hyperpolarizes during sustained light, owing to a drop in the potassium concentration in the interphotoreceptor space (Oakley, 1977, 1983; Steinberg et al., 1980). RPE cells maintain an apical-side–positive transepithelial potential of 8–20 mV in the frog (Miller and Steinberg, 1977), 20–30 mV in the toad (Lasansky and De Fisch, 1966), and 5 mV in the dog (Tsuboi et al., 1986), which is affected by external and internal ion concentrations (Miller and Steinberg, 1977) and (indirectly) by light (Oakley, 1977; Oakley et al., 1978; Steinberg et al., 1980, 1983; Miller and Steinberg, 1982; Griff and Steinberg, 1982; Linsenmeier and Steinberg, 1982, 1983).

We have recorded from human RPE cells obtained from donor eyes taken at autopsy. These cells can be grown in culture, where they proliferate as flat cells that continue to produce pigment granules and apical processes (Pfeffer et al., 1986). In this report, we describe the properties of the main types of channels observed in recordings from the exposed (apical) surfaces of cultured human RPE cells. There are at least three potassium-selective channels, with on-cell slope conductances (with tissue culture medium in the pipette) of 100, 45, and 25 pS, and one nonselective channel, with an on-cell slope conductance of ~300 pS. The 100- and 25-pS potassium-selective channels are the most frequently observed. This is consistent with Miller and Steinberg's (1977) finding of a large potassium permeability in the apical membrane of frog RPE. Some of this work has been described previously at the annual meetings of the Society for Neuroscience, the Association for Research in Vision and Ophthalmology, and the Biophysical Society (Fox et al., 1984, 1985, 1986).

METHODS

Cell Culture

RPE cells collected from human donor eyes obtained at autopsy were cultured as previously described (Pfeffer et al., 1986). The ages of the donors at the time of death ranged from 8 mo postnatal to 30 yr. Cells were grown on gelatin-covered glass coverslips cemented with wax to the bottom of plastic culture dishes.

Solutions

The tissue culture medium used was Dulbecco's modified Eagle's medium (DMEM) plus medium 199 (1:1), or in some cases, DMEM alone (Gibco, Grand Island, NY). The ionic composition of DMEM plus medium 199 was (in millimolar): 148 Na, 5.6 K, 1.6 Ca, 1.3 Mg, 131.6 Cl, 24.1 HCO_3, 0.8 SO_4, 0.7 H_2PO_4, 0.15 HPO_4, and 5.6 glucose at pH 7.2–7.4. DMEM alone contained 154.4 mM Na, 1.8 mM Ca, and 117 mM Cl, but had the same K, Mg, and glucose concentration as DMEM plus medium 199. In most experiments, the tissue culture medium was removed and replaced with another solution. In many experiments, the replacement medium was minimum essential medium (Gibco) with Hanks' salts with 25 mM HEPES. This solution contained (in millimolar): 141.7 Na, 5.8 K, 0.95 Ca, 0.89 Mg, 145.14 Cl, 4.17 HCO_3, 1.1 H_2PO_4, and 0.41 SO_4. Occasionally, Konigsberg's solution was used. This solution consisted of (in millimolar): 129 Na, 4.55 K, 0.7 Mg, 1.1 Ca, 135 Cl, 0.2 SO_4, 1.4 H_2PO_4, pH 7.2–7.4. All single-salt solutions, such as 0.1 M NaCl or 0.1 M KCl, were buffered with 10 mM HEPES to pH 7.2. Serum was not present in the solutions, as it seemed to inhibit seal formation. In some experiments, the patch pipette was filled with a high-potassium solution to mimic intracellular ionic conditions. This solution, referred to in the text as potassium internal solution, consisted of (in millimolar): 100 KCl, 10 NaCl, 2 $MgSO_4$, 5.5 EGTA-KOH, 0.5 $CaCl_2$ (for a free calcium concentration of 10^{-8} M), and 10 HEPES, pH 7.2. This solution was intended to resemble the cell interior as closely as possible.

All recordings were performed at room temperature (22°C), with the dishes exposed to air. At this temperature, the channel conductance would not be much affected, though the channel kinetics might be slowed from the values that would be found at 37°C (Hille, 1975). Since the medium in some early experiments contained high bicarbonate concentrations and the dishes were not bubbled with CO_2 (to prevent mechanical disruption of the seals), some rise in bath pH (0.5–1 pH unit) typically occurred during the course of these experiments. To prevent the pH from rising excessively, we exchanged the medium (as described above) in most experiments with HEPES-based solutions. The recording time from cells in a plate was generally limited to 1–3 h.

Electrodes

The electrodes used were micro-hematocrit capillary tubes (75 mm long × 1.1–1.2 mm o.d.; wall thickness, 0.2 mm; Van Waters and Rogers, Norwalk, CA), pulled by the double-pull method of Hamill et al. (1981) with a vertical puller (David Kopf Instruments, Tujunga, CA). The walls of the pipettes were coated with Sylgard (Dow Corning Corp., Midland, MI) to reduce capacitance. The pipette tips were fire-polished. Illumination for fire-polishing was provided by shining a light from a fiber-optic light pipe down the length of the pipette, causing the pipette tip to glow (Fox, 1985). The pipette resistance was typically 2–5 MΩ, indicating a tip size of 0.5–1 μm (Hamill et al., 1981). Pasteur pipettes filled with a 2% agar-Ringer's solution were used as a ground in the bathing medium.

Electronics

Ion channel currents were amplified by an ultrahigh-gain amplifier (EPC-7, List Medical Systems, Great Neck, NY), monitored by an oscilloscope, and recorded continuously on FM tape. Two tape recorders were used during the course of the experiments. A Tandberg Series 100 instrumentation tape recorder (Tandbergs Radiofabrikk, Oslo, Norway) was used for ~75% of the experiments, with the remaining experiments being recorded with a Hewlett-Packard 3960A instrumentation tape recorder (Hewlett-Packard Co., Palo Alto, CA). Output from the Tandberg recorder was filtered with a five-pole transitional Thompson-Butterworth filter with a −3-dB point of 2,777 Hz. The −3-dB point for the Hewlett-Packard recorder was 5,252 Hz. FM records were subsequently digitized at a sampling rate of 10 kHz and stored on disk for later analysis on a MINC 11-23 minicomputer (Digital Equipment Corp., Marlboro, MA).

Data Analysis

The data analyzed were records of single-channel activity at a constant potential. These records were typically 5 s in duration (range, 1.5–24 s). Before analysis, records were digitally filtered with a smoothing routine. The smoothing routine added the values of adjacent pairs of data points and replaced the first value of the pair with half the sum (Mejia and Chang, 1970). This digital filtering will reduce the signal amplitude by −3 dB at a frequency that is determined by the sampling rate and by the number of iterations of the procedure. Six iterations of this smoothing routine were commonly applied. Our data were sampled at 10 kHz, so that the −3-dB frequency for six iterations of this routine was 1,071.5 Hz. Eight iterations resulted in a −3-dB point of 833 Hz.

The data on disk consisted of the value, at each sample time, of the current flowing across the membrane under the patch electrode. The single-channel amplitude was determined by creating a histogram, with membrane current as the abscissa and the number of sample points for membrane current in each of the equally sized bins as the ordinate (see Labarca et al., 1984). Such histograms have peaks centered at the zero-current level and at the current levels corresponding to one, two, etc., open channels. The position of a peak was determined by the bin (near a cursor that had been set by eye) that had the largest number of points. The single-channel current was found from the difference between any two adjacent peaks. An experimental record and the amplitude histogram created from that record are presented in Fig. 1.

Kinetic Analysis of Single-Channel Events

The patch-clamp record shown in Fig. 1 *A*, containing single and multiple channel opening events, illustrates the methods used to determine single-channel open times. Cursors were set to the open- and closed-current levels on an oscilloscope display of the digitized data record. These levels were determined either by eye or from the peaks found in amplitude histograms such as the one shown in Fig. 1 *B*. The current level nearest to zero membrane current was taken as the closed level. This level generally had the lowest noise. The setting of the open and closed levels automatically set a threshold level at 50% of the open-channel current (Colquhoun and Sigworth, 1983). Channels were considered open at a membrane current greater than the threshold level for potentials at which the open-channel current was positive. The same procedure was followed for negative open-channel currents, but the designations of open and closed were reversed. Our analysis routine correctly identified above-threshold transitions when tested with noisy artificial data.

Single-channel patches. In patches without simultaneous multiple openings, as determined from amplitude histograms, the open time was determined from the number of sampling intervals between the first open data point and the next closed data point, and vice versa for closed times. The average open time was calculated by dividing the sum of

all the open times by the number of closures. In stretches of data with no transitions, small amounts of drift were accommodated by using the difference between the previous current level and the average of the 10 subsequent data points to adjust the threshold (Colquhoun and Sigworth, 1983).

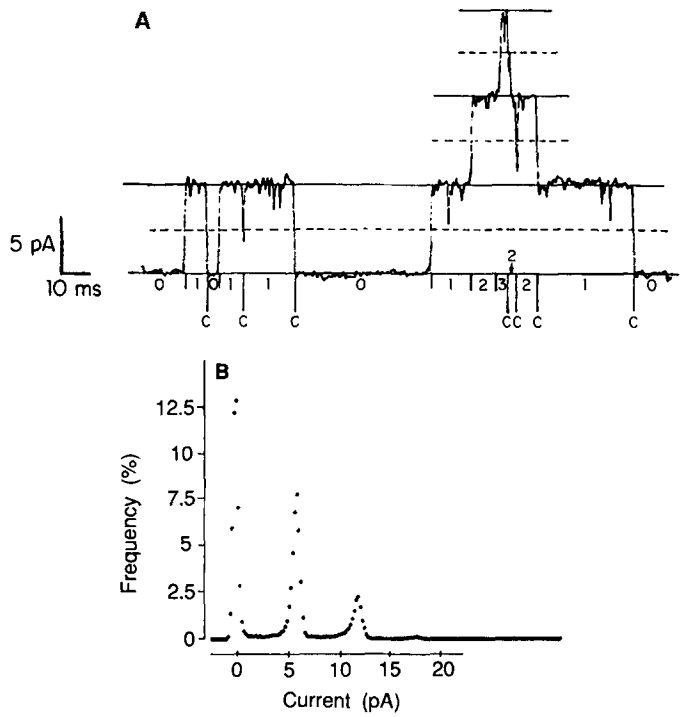

FIGURE 1. (*A*) Single-channel currents from an on-cell membrane patch containing several channels of the 100-pS potassium-selective type. The pipette contained potassium internal solution. This record illustrates the features used by the data analysis programs to determine channel open and closed times. Openings are upward in this record. Levels corresponding to the current due to zero, one, two, and three open channels are drawn with solid lines. The zero-current level is the baseline used to determine the number of open channels in multichannel patches. Threshold levels equal to half the open-channel current are drawn with dashed lines. Channel closing events, defined as transitions in which the membrane current drops below a threshold level, are marked at the bottom of the figure with the letter "C." The numbers just below the zero-current level indicate the numbers of channels open in the corresponding time segment. In this and subsequent figures, outward current is plotted upward and potential is the negative of the pipette potential. The recording bandwidth was 0–2,777 Hz; the record was digitally smoothed with a corner frequency of 1,071.5 Hz (see Methods). (*B*) Amplitude histogram created from the record shown in *A*. The histogram was constructed by summing the sample points at each membrane current (see Methods).

Histograms. In records with only one active channel in a patch, open- and closed-time histograms were constructed. The determination that a patch contained only a single channel was made if no double openings were observed in a record of several seconds'

duration in which the channel was open most of the time. This condition was met in only 5 of the 86 patches with channel activity.

The histograms of open and closed times were then fitted with single or double exponentials. The best-fitting (single or double) exponential curve was determined using the simplex minimization procedure of Nelder and Mead (1965).

This curve-fitting procedure was verified in the following way. Idealized single-channel events were written to a data file in arbitrary sequence. The number of idealized openings and closings of a particular duration was determined from double-exponential distributions with decay constants of 5 and 50 points for the high current level, and 8 and 60 points for the low current level. Our data analysis program determined that the best-fitting parameters for these artificial data were 5 and 49.29 for the high current level, and 7.94 and 59.94 for the low current level.

Multichannel patches. Open and closed levels were set as for single-channel patches to designate the open-channel current and so determine the 50% threshold level. In addition, a third cursor was set to the baseline current level, the lowest current level observed in the record (see Fig. 1 *A*). This baseline level was the membrane current with the fewest open channels, and in most cases it was very close to the zero membrane current level, which indicates that all channels in the patch were closed. The threshold was initially set at half the open-channel current above the baseline. Current exceeding threshold caused the threshold to be iteratively increased in steps the size of the open-channel current until the new threshold was greater than the experimental current. The number of iterations gave the number of channels open in the patch. Subsequent increases or decreases in current of >50% of the open-channel current were taken to be increases or decreases in the number of channels open and caused a corresponding adjustment of the threshold by an amount equal to the open-channel current. For experiments in which the open-channel current was negative, the designation of open and closed was reversed and the baseline was set accordingly.

Average channel open time. For patches with more than one active channel of a single type, the average channel open time was calculated by summing the total open time (weighted by the number of channels open at each time point) and dividing by the number of closures (Fenwick et al., 1982; Benham and Bolton, 1983; Horn et al., 1984). The number of active channels in a patch need not be known to use this method, as long as the zero-current level is known. When applied to channels with only one open state, the average open time calculated by this method yields the maximum-likelihood estimate of the open-channel lifetime (Horn et al., 1984). Since our best exponential fittings imply more than one open state for the channels we observe (see Results), the average open times we calculate may not be the maximum-likelihood estimates of the open time. However, this method provides objective estimates of the average channel open time, which can be used to characterize our data and to compare results from different experiments.

We tested the analysis program used in these calculations against manufactured data for a membrane with three active channels, with an aggregate average open time of 85.52 ms for 898 channel closing events. The program calculated an average open time of 85.49 ms for 898 observed closures.

Probability of a channel being open. The probability of a channel being open (P_o) was determined from the fraction of time spent in the open state for patches with only one channel. This fraction was found by dividing the total open time in a record by the duration of the entire record. In patches with more than one active channel of a single type, we calculated the fraction of time spent with no channels open, or with one, two, and so on. The fraction of time spent at a given current level was determined from the

sum of the time spent at that level divided by the total time in the record. P_o was found by fitting these fractions with the binomial theorem (Ohmori et al., 1981; Patlak and Horn, 1982; Benham and Bolton, 1983).

We tested the program that determined these values by using it to analyze an idealized current record that mimicked the current levels that might be observed in a patch with three independent channels of equal amplitude, each with an open probability of 0.5. The fraction of sample points, determined by the binomial distribution, was 0.125 at the lowest current level, 0.375 at the next, also 0.375 at the next higher, and 0.125 at the highest current level. The analysis program reported that the fractions of time spent with zero, one, two, and three channels open were 0.125, 0.375, 0.375, and 0.1248. The best fitting of these values to the binomial theorem gave a channel open probability of 0.5 for three channels present in the patch.

The fractions of openings at each current level could also be determined from the areas under the peaks in amplitude histograms such as the one shown in Fig. 1*B*. The area under a peak was found by summing the amplitudes of the points around the peak. The point between two peaks with the smallest amplitude was used to separate adjacent peaks. If the minimum point was zero, the midway point between the peaks determined the separation. The area under a peak divided by the total area in the histogram gave the probability of the patch being in that state. This method gave results similar to those obtained by the method described above and was used as an independent check of the validity of our determinations of P_o.

RESULTS

RPE cells, like other cells in culture (Taub, 1984), express membrane differentiation in vitro that is similar to that found in vivo, with the cell surface that faces the bath corresponding to the apical membrane (Crawford, 1983). In confluent cultures of the cells used in our experiments, RPE cell polarization was indicated by the presence of villi (Pfeffer et al., 1986) and Na,K-ATPase (Pfeffer, B. A., J. Usukura, W. O'Day, and D. Bok, manuscript in preparation) at the cell surface exposed to the culture medium, and by basal infoldings found at the opposite (basal) membrane in contact with the culture dish and supporting gelatin (Pfeffer et al., 1986). Fig. 2 is a photomicrograph that shows a subconfluent group of human RPE cells in culture. Most of our recordings were from cells in subconfluent dishes, since we seemed to have greater success in forming gigohm seals under these conditions.

Approximately 80% of the membrane patches recorded from the cell surface facing the bath showed channel activity on-cell after the formation of seals with resistances >1 GΩ. In most cells, this activity could be observed at the normal resting potential (i.e., with the pipette potential at ground). The remaining 20% of our gigohm seals showed no single-channel current steps at any applied voltage, even after repeated passage of the pipette with the membrane patch into and out of the bath solution to preclude the possibility of membrane vesicle formation (Hamill et al., 1981).

Our results are based on examinations of single-channel activity observed in 35 on-cell and 51 excised-membrane patches. Of these patches, <6% could be shown to contain only one channel. Patches containing more than one channel usually appeared to contain channels all of the same type, as if the channel types clustered in the RPE cell membrane. Channel clustering has also been observed

in the membranes of other ocular epithelia (Rae and Levis, 1984*b*). Approximately 20% of the patches had activity caused by more than one type of channel.

We used measurements from both excised and on-cell patches to characterize the observed channels. Channel conductance was determined from the single-channel amplitude by determining the slopes of single-channel current-voltage relations. Channel selectivity was determined from reversal potential measurements from patches bathed with solutions of different ionic compositions at the two membrane faces.

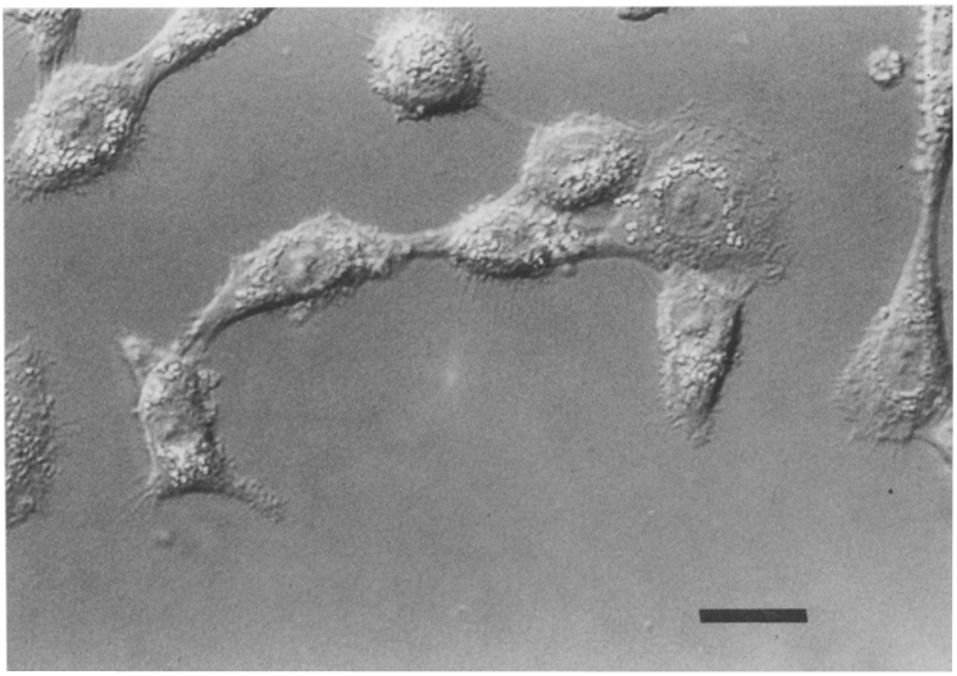

FIGURE 2. Nomarski micrograph of human RPE cells in tissue culture made on a Zeiss Invertoscope D microscope. A subconfluent dish is shown here, since most recordings were made from such preparations. However, recordings were also made from dishes at various densities up to and including confluency (see Methods). The scale is 20 μm.

Initially, we sought to determine whether the channel activity that we observed could be grouped into distinct classes of different channel types. Comparison of slope conductances determined from single-channel amplitudes observed under equivalent experimental conditions is a convenient way to begin to perform this grouping. Further classification of the ionic selectivity and kinetic properties of the channels can then be made, using this initial division as its basis. From such measurements, we have classified the channels observed in our recordings into at least four main types, consisting of at least three potassium-selective channels, which we term (in order of the single-channel conductances) large, medium, and small, and a large-conductance nonselective channel. Large potassium-selective channels were observed in 40% of the patches with channel activity, medium

potassium channels in 15%, and small potassium channels in 30%. The large nonselective channel was observed in 10% of the patches with channels.

Approximately 15% of the patches had some channel activity that could not be identified as belonging to one of these four groups. In some cases, insufficient data were collected before loss of the seal, preventing the confident classification of the data into one of the amplitude groups. However, in other cases, our observations indicate the existence of one or more rare channel types that we have not yet been able to investigate in detail.

Potassium Channels

Large potassium-selective channel. This channel was the most commonly occurring channel in the patches we examined. For this reason, we were able to measure its single-channel properties under several experimental conditions.

Examples of single-channel currents and the corresponding current-voltage plots from patches containing large potassium-selective channels are presented in Fig. 3. Fig. 3*A* illustrates single-channel currents from an on-cell patch with medium in the pipette. The slope conductance calculated from the current-voltage plot shown in Fig. 3*B* was 90 pS, and the negative of the pipette potential at which the current reversed was −24 mV. The channel currents in Fig. 3*C* were from an on-cell patch with the pipette filled with potassium internal solution. The slope conductance calculated from the corresponding current-voltage curve (Fig. 3*D*) was 110 pS, and the negative of the pipette potential at which current reversed was 60 mV.

In order to translate these values for on-cell reversal potentials into transmembrane potentials, the resting membrane potential of these cells must be determined. This was done in separate experiments in several culture dishes by sealing a pipette filled with potassium internal solution to an isolated cell, then breaking through the cell membrane into the whole-cell configuration, and immediately thereafter noting the potential under current clamp. The average resting potential was found to be −44 ± 8 mV (mean ± standard deviation) for 23 cells. Thus, the transmembrane reversal potential obtained from the experiment with medium in the pipette (Fig. 3, *A* and *B*) was approximately −68 mV, while that from the experiment with internal solution in the pipette (Fig. 3, *C* and *D*) was approximately +16 mV.

A more complete summary of our measurements on the large potassium-selective channel is given in Figs. 4 and 5, which combine the results of several experiments into individual current-voltage plots. Although some recordings in different experiments did not cover the full voltage range shown in the plots, we classified data with similar slope conductance and apparent reversal potentials together.

Fig. 4*A* is a plot of the current as a function of the potential through the large potassium-selective channel observed in six on-cell patch experiments with medium in the pipette. Each different symbol represents a separate membrane patch. The mean slope conductance found for the six experiments shown in Fig. 4*A* was 99 ± 19 pS, with a mean reversal potential of −16 mV. Combining this reversal potential with the mean resting potential of −44 ± 8 mV (see above),

we calculate the transmembrane potential at which the current reverses to be approximately −60 ± 8 mV. This value is consistent with potassium-over-sodium selectivity for this channel. However, since the intracellular ion activities of human RPE cells have not been measured, the permeability ratio, P_K/P_{Na}, cannot be calculated from these measurements. Furthermore, it was not possible to compensate our measured resting potential values for junction potentials between the pipette solution and the cell interior, since we had no way of estimating the

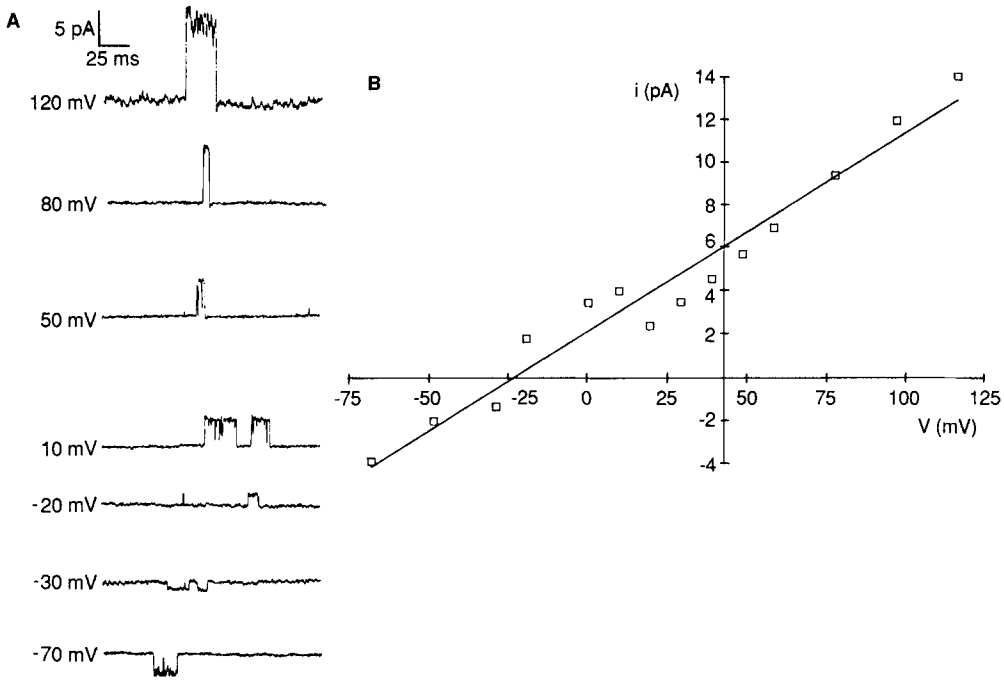

FIGURE 3. Single-channel current records from intact human RPE cells. Large potassium-selective channel. (*A*) On-cell patch, medium in the pipette. (*B*) Current-voltage plot of the currents shown in *A*. Channel currents are plotted vs. the negative of the pipette potential. The slope conductance was 89.99 pS and the reversal potential was −24 mV (calculated transmembrane potential, −68 mV). (*C*) On-cell patch, potassium internal solution in the pipette. (*D*) Current-voltage plot from the patch shown in *C*. The slope conductance was 110 pS and the reversal potential was 60 mV. The recording bandwidth for both sets of channel records was 0–2,777 Hz; the record was digitally smoothed with a corner frequency of 1,071.5 Hz.

value of the offset. Measurements by other investigators (Marty and Neher, 1983; Fernandez et al., 1984) indicate that our value for the reversal potential could be as much as 10 mV too positive (i.e., the reversal potential may be as low as −70 mV).

In Fig. 4*B*, we present a current-voltage plot for five experiments with the large potassium-selective channel observed in on-cell patches with potassium internal solution in the pipette. In this situation, there should be nearly symmetric

ionic concentrations across the membrane patch. The mean slope conductance was 115 ± 13 pS, with a mean reversal potential of 53.4 mV. Using our value for the average cell resting potential, this corresponds to a transmembrane potential of 9.4 ± 8 mV. This is approximately the potential expected for a potassium-selective channel under these conditions.

In Fig. 5*A*, we plot single-channel currents as a function of voltage for the large potassium channel observed in eight excised, inside-out patches. With potassium internal solution in the pipette and medium in the bath, the mean slope conductance was 97 ± 16 pS and the mean reversal potential was 51 mV. By using the Goldman-Hodkin-Katz equation (Hille, 1975) with known ionic concentrations at both membrane faces, the P_K/P_{Na} determined from these eight

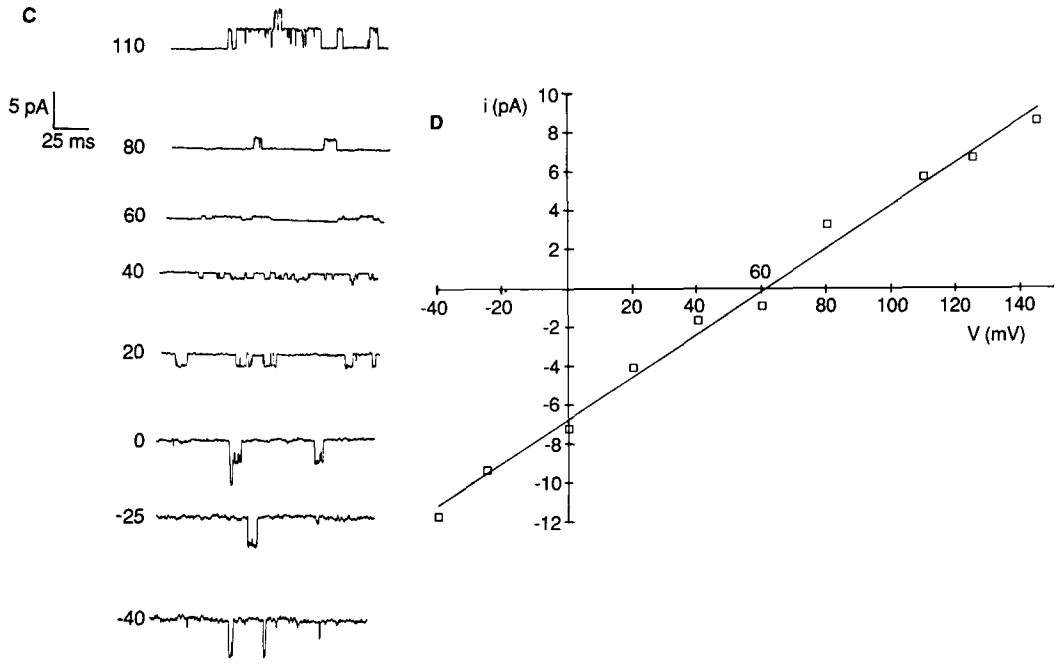

FIG. 3, *C* and *D*.

experiments, plus three other excised-patch experiments with slightly different sodium and potassium concentrations, was 21 ± 12.

We measured the single-channel reversal potential when a KCl concentration gradient was imposed across the membrane patch in order to determine the potassium-over-chloride ion selectivity. Fig. 5*B* shows a graph of single-channel current vs. potential for the large potassium-selective channel in two separate patches bathed with 0.5 M KCl on the cytoplasmic face and with 0.2 M KCl on the extracellular face. The regression line fitted to the channel openings for outward current flow gives a slope conductance of 269 pS and a reversal potential of −18.7 mV. Note that the unitary conductance was higher than in previous measurements, since the potassium concentration was higher (see *Channel Con-*

ductance as a Function of Ion Concentration below). The two data points for inward current could be fitted separately with a regression line (not shown) crossing the voltage axis at approximately the same reversal potential as for the outward currents. The calculated Nernst potential for potassium under these conditions is −20.6 mV. From the reversal potential we observed, we calculated a P_K/P_{Cl} of 23.3.

In some patches, both inward and outward currents were observed for the large potassium-selective channel as the pipette potential was varied (see Fig. 3). However, in other patches, clear single-channel steps were observed for current

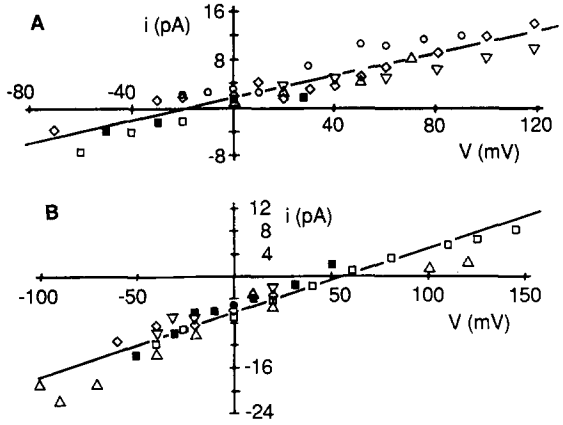

FIGURE 4. (*A*) Current-voltage plot of the results of six experiments in which the large potassium-selective channel was observed in on-cell patches with the pipette filled with medium. The mean slope conductance was 99 pS, with current reversing at −16 mV, corresponding to a transmembrane potential of approximately −60 mV. See text. (*B*) Current-voltage plot for the large potassium-selective channel observed in five separate on-cell experiments with potassium internal solution in the pipette. In this situation, there should be nearly symmetric ionic concentrations across the membrane patch. The mean slope conductance was 115 pS and the mean reversal potential was −53 mV (corresponding to an approximate transmembrane potential of 9 mV). Lines are linear regression fittings to all data points in both *A* and *B*.

flowing in one direction only, either because the concentration of permeant ions was small on one side of the membrane, or because P_o declined at large positive or negative potentials. Although these observations could be interpreted as evidence for separate populations of inwardly and outwardly rectifying channels in some of our recordings, the simplest explanation of our results is that the same population of nonrectifying channels was observed in all of our experiments.

Kinetics of the large potassium-selective channel. Open- and closed-time histograms were created for patches that contained only a single active channel. We

found, in general, that double-exponential fittings to open- and closed-time histograms gave smaller squared errors than did single-exponential fittings. The time constants obtained from these fittings from one patch are shown plotted as a function of transmembrane potential in Fig. 6. The fast time constants showed very little variation with membrane potential, but more variation was seen for the slow time constants. The slow time constant for open times reached a maximum value near the cell resting potential, while the slow time constant for closed times was greatest at the most hyperpolarized potential and declined slightly with depolarization at other potentials.

Most of the patches containing the 100-pS potassium-selective channel contained more than one of these channels. Although in this case an open-time histogram could not be constructed (Colquhoun and Sigworth, 1983), it was possible to calculate an average channel open time, as described in the Methods.

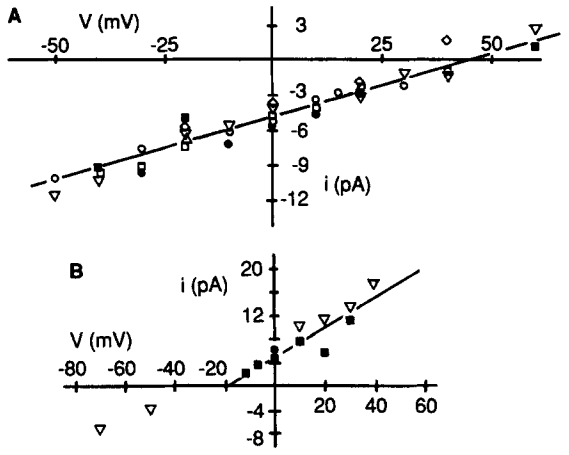

FIGURE 5. (*A*) Current-voltage plot for the large potassium-selective channel from eight excised, inside-out membrane patches bathed with medium at the cytoplasmic face and potassium internal solution at the extracellular face. Positive potential on the graph is equivalent to depolarization of the patch. The mean slope conductance was 97 pS and the reversal potential was 51 mV. The linear regression line to all data points is shown. (*B*) Current-voltage plot for the large potassium-selective channel in two separate excised patches bathed on the cytoplasmic face with 0.5 M KCl and on the extracellular face with 0.2 M KCl. The reversal potential indicates high potassium-over-chloride selectivity. The linear regression line is for both sets of data points for outward currents only.

The average open times of the large potassium-selective channel are presented in Fig. 7, *A* and *B*. The average open times of the patch presented in Fig. 6 are represented in Fig. 7*A* by filled triangles. In several on-cell patches (Fig. 7*A*), the average open time peaked near the cell resting potential (i.e., 0 mV pipette potential). This voltage-dependent behavior was similar to the voltage-dependent behavior of the slow open time constant (Fig. 6*A*). However, not all patches exhibited this potential dependence. The average open time in some patches showed only small variation with potential (squares, crossed squares). In two patches, the average open time increased with depolarization (diamonds, circles).

The average open time in excised-patch experiments was also variable (Fig. 7*B*). In the patch represented by the circles, the average open time peaked near rest, and in two other patches (triangles, diamonds), the average open time

declined as the patch was depolarized from rest. However, in the patch represented by triangles, the average open time was high at both +40 and −40 mV, and so did not continuously decline with depolarization. In other patches, the average open time increased with depolarization, and in two patches, it showed little variation over the experimental range of potential.

The average channel open time gives an estimate of the mean channel closing rate. A more complete description of the kinetic behavior of a channel would include some measure of both open and closed times. The probability of a channel being open (P_o) at a given voltage is one such measure. P_o for the 100-pS potassium channel is presented in Fig. 7, *C* and *D*, as a function of transmembrane potential. The results from on-cell experiments are presented in Fig. 7*C*, including P_o for the single-channel patch analyzed in Fig. 6 (filled triangles). The decline in P_o with hyperpolarization in this patch is consistent with the decline of the slow open time constant and the increase of the slow closed time constant with hyperpolarization shown in Fig. 6. This patch and one other (crossed

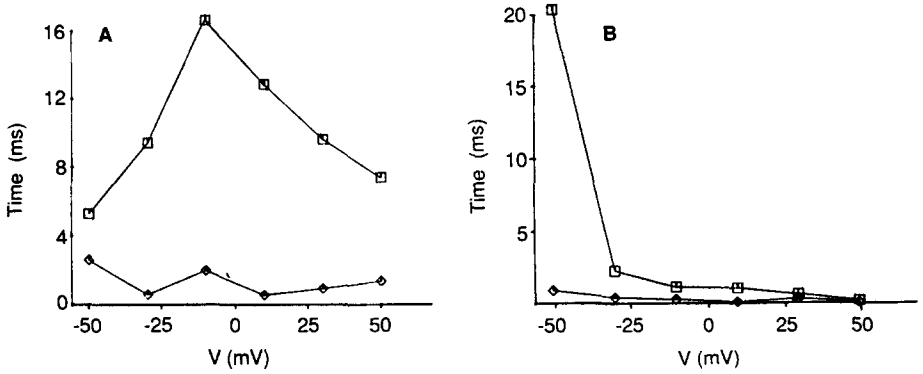

FIGURE 6. Fast and slow time constants fitted to histograms from the patch in Fig. 3*A*. (*A*) Open times; (*B*) closed times.

squares) had high values of P_o near the resting potential. P_o for the channels in the patch represented by the hourglass symbols was near unity at potentials near rest (0 mV applied) and at 50 and 70 mV (negative pipette potential), while channels in one patch (circles) had a maximum P_o of 0.25 at 60 mV negative pipette potential. Two patches had low values at all potentials, although these did peak near 0 mV (diamonds, squares). P_o from excised-patch experiments (shown in Fig. 7*D*) also showed no clear general trend with potential, although in data from one patch (crossed squares), P_o clearly increased as the patch was depolarized. When P_o at each potential was plotted in the sequence at which the potentials were applied, no apparent periodicity was found (data not shown).

The average open time and P_o were variable from patch to patch in both on-cell and excised-patch experiments, though the range of values from a single patch tended to be larger for the cell-attached patches. In one excised patch, where the average open time and P_o were remeasured under identical conditions at several potentials ~5 min after the first measurements and after having

undergone two solution changes, the initial and final average open-time values were similar, in both cases declining somewhat with depolarization of the patch. The P_o values were also similar at many, but not all, potentials (circles and crosses, Fig. 7, *B* and *D*). This suggests that the kinetic parameters of channels in a given patch were for the most part stable during the time course of our recordings. However, abrupt changes in kinetic activity at constant potential in a single patch have also been observed. For example, a large potassium-selective

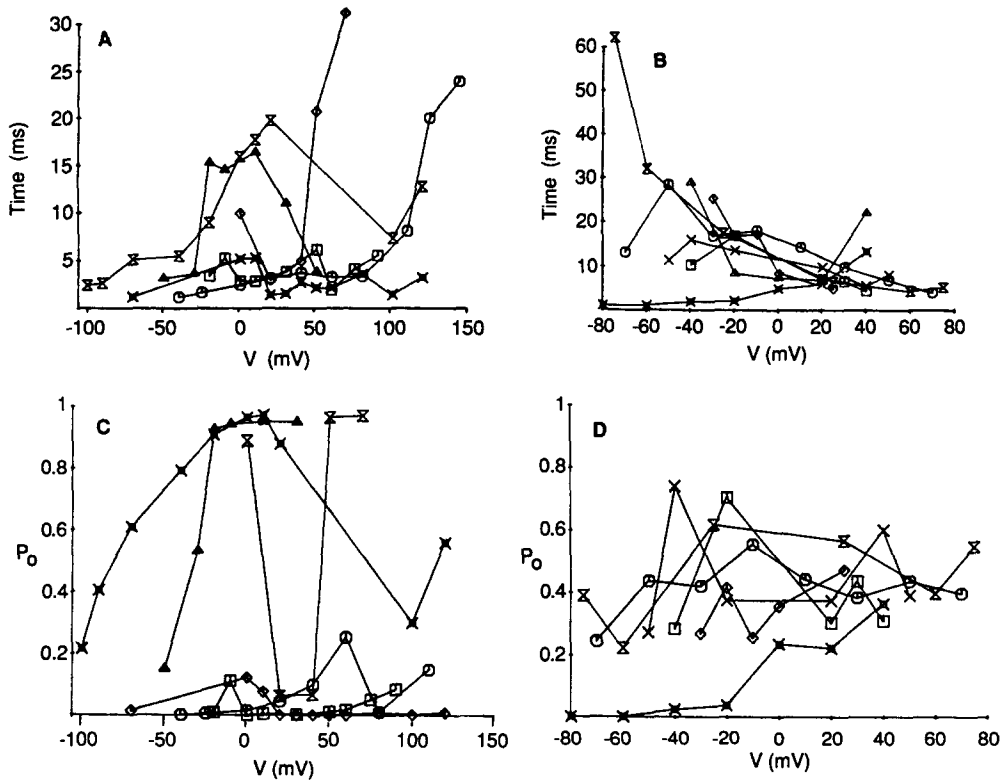

FIGURE 7. (*A*) Average open times from on-cell patches. (*B*) Average open times from excised, inside-out patches. Lines connect measurements from a single patch. (*C*) P_o of the large potassium-selective channel plotted vs. negative pipette potential from on-cell patches. (*D*) P_o from excised patches. P_o was found by fitting the fraction of time that the patch current was observed at each current level to the binomial theorem (see Methods). The filled triangles in *A* and *C* are data from the patch in Fig. 6.

channel, observed at one potential for >13 s, was active, with P_o >0.5 for 10 s, but twice it shut completely for >1 s before resuming activity at the previous level. Such behavior was noted in records from at least one applied potential in ~40% of the patches with active channels of the 100-pS potassium-selective type.

Medium potassium-selective channel. Channels having a unitary conductance of ~45 pS were the least commonly observed type of potassium channel. The records shown in Fig. 8, *A* and *B*, illustrate two examples of these channels, with

the corresponding current-voltage curves shown in Fig. 8*C*. In these experiments, channels were observed in excised, inside-out patches with 0.1 M NaCl in the bath and 0.1 M KCl in the pipette. The slope conductance for the channel in Fig. 8*A* was 45 pS, with a reversal potential of 26 mV. The calculated permea-

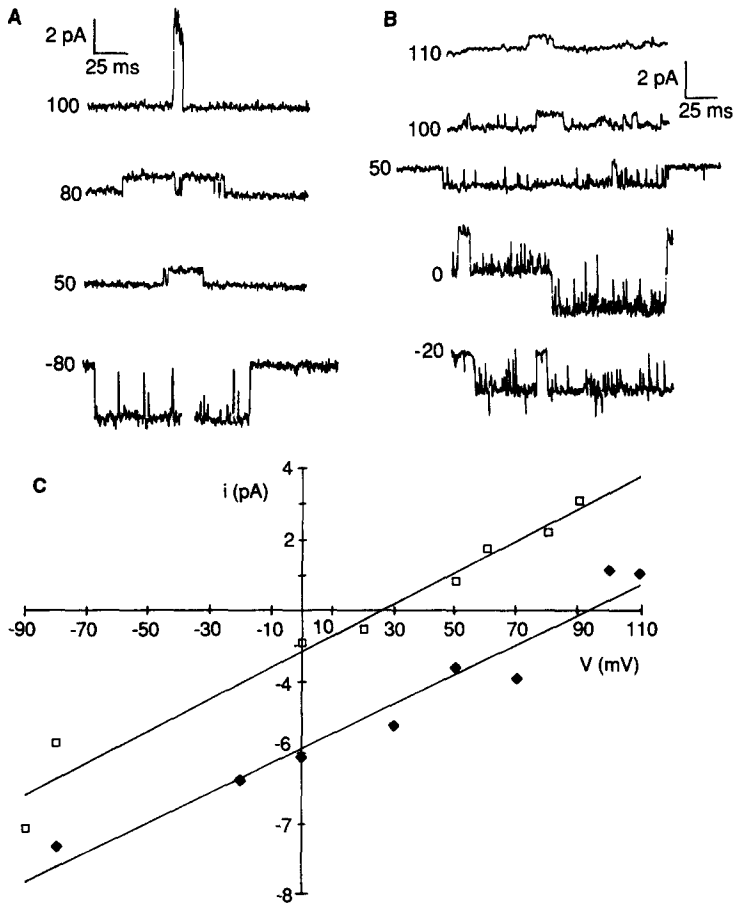

FIGURE 8. (*A*) Single-channel currents from the medium potassium-selective channel in an excised inside-out patch with 0.1 M KCl in the pipette and 0.1 M NaCl in the bath. The slope conductance was 45 pS and the reversal potential was 26 mV. A portion of the record without transitions was deleted from the bottom trace. (*B*) Single-channel currents from a different excised patch under identical conditions. The slope conductance was 42 pS and the reversal potential was 93 mV. The recording bandwidth for both sets of records was 0–2,777 Hz; records were digitally smoothed with a corner frequency of 1,071.5 Hz. (*C*) Current-voltage plot of the single-channel activity in the patches in *A* (squares) and *B* (diamonds).

bility ratio, P_K/P_{Na}, was 2.9. In the other example of a medium-conductance potassium channel, shown in Fig. 8*B*, the slope conductance was 42 pS, the reversal potential was 93 mV, and the permeability ratio was 41. In two excised, inside-out patches with asymmetric potassium and sodium ion concentrations across the membrane, a slope conductance of 44 ± 1 pS and a P_K/P_{Na} of 2.7 ±

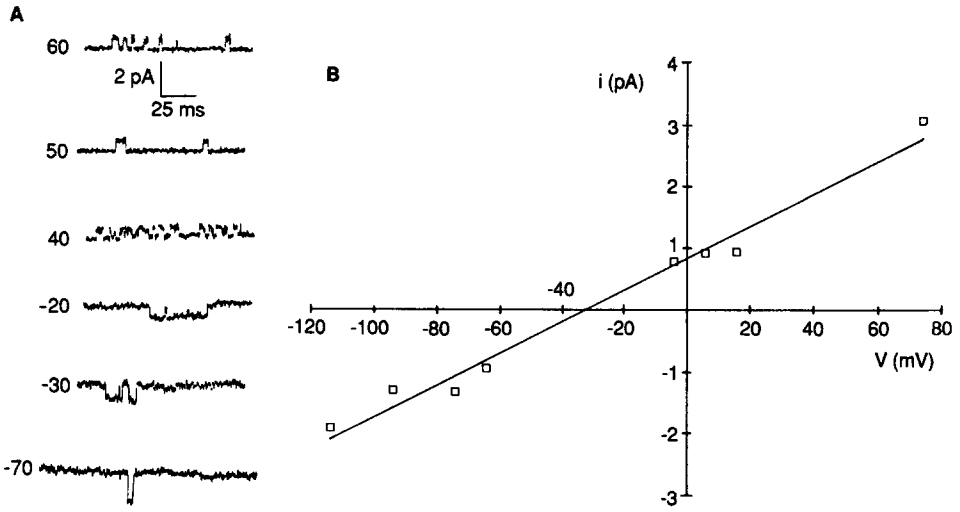

FIGURE 9. (*A*) Single-channel currents of the small potassium-selective channel from an on-cell patch with medium in the pipette. The recording bandwidth was 0–2,777 Hz; records were digitally smoothed with a corner frequency of 1,071.5 Hz. (*B*) Current-voltage plot of the single-channel activity from the patch in *A*. The slope conductance was 26 pS and the reversal potential was 12 mV (estimated transmembrane potential, −32 mV.

0.3 were found. In two other patches under the same conditions, the average slope conductance was 44 ± 2 pS and the P_K/P_{Na} was 40.7 ± 0.4. These results indicate at least two populations of potassium channels with similar conductances.

Channels with similar slope conductances were also observed in on-cell experiments. The mean slope conductance from three on-cell experiments with medium in the pipettes was 45 ± 1 pS, while that from three on-cell experiments with internal solution in the pipette was 44 ± 2 pS.

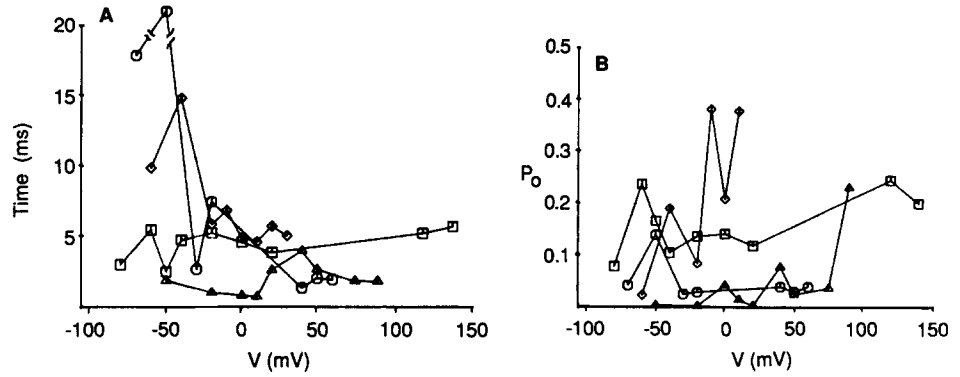

FIGURE 10. (*A*) Average open time of the small potassium-selective channel in on-cell patches as a function of negative pipette potential. The circle at −50 mV, which is offscale, represents an open time of 55 ms. (*B*) P_o of the 25-pS potassium-selective channel observed in on-cell patches vs. membrane potential. Data from single patches are connected by lines.

Since relatively few recordings were made from medium potassium-selective channels, and since there were probably at least two kinds of such channels, no attempt was made to give an analysis of their kinetic properties.

Small potassium-selective channel. The second most commonly observed channel was the smallest of the potassium-selective channels, which had a unitary conductance of ~25 pS. Recordings from this type of channel are illustrated in Fig. 9*A*, with a corresponding current-voltage plot shown in Fig. 9*B*. The slope conductance of the channel in Fig. 9 was 26 pS. In excised, inside-out patches

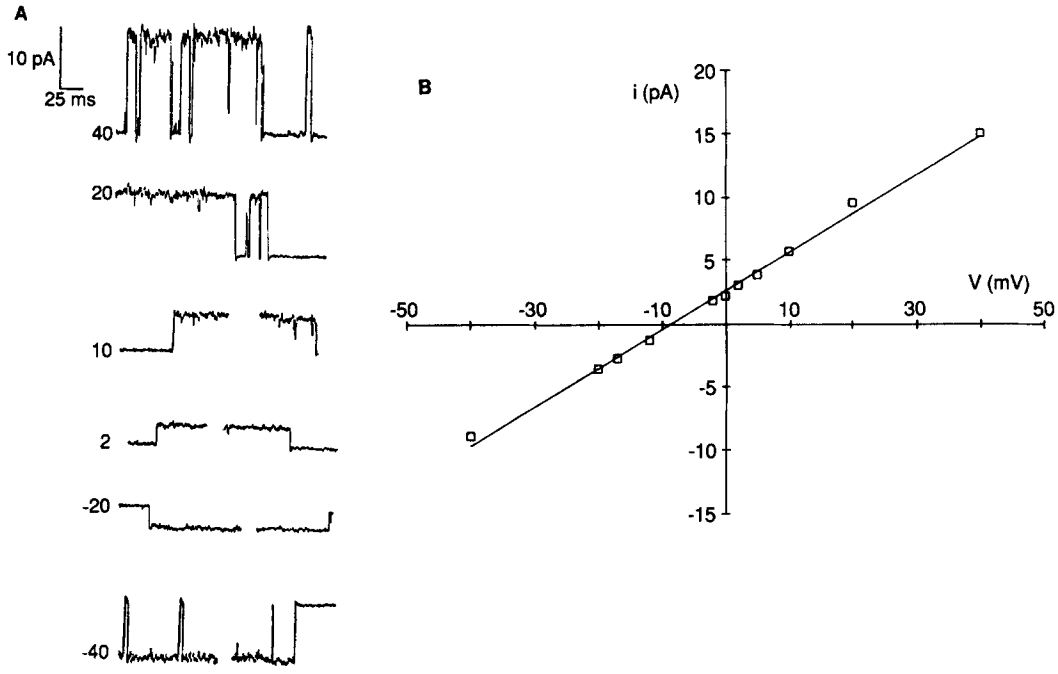

FIGURE 11. (*A*) Single-channel records of the large nonselective channel from an excised inside-out membrane patch bathed with 0.1 M NaCl in the bath and 0.1 M KCl in the pipette. The recording bandwidth was 0–2,777 Hz; records were digitally smoothed with a corner frequency of 1,071.5 Hz. Gaps in records indicate portions without transitions, which have been deleted. (*B*) Current-voltage plot from this patch. The slope conductance was 306 pS and the reversal potential was −9 mV, giving a calculated P_K/P_{Na} of 0.7.

with asymmetric sodium and potassium ion concentrations across the membrane, the small potassium channel recorded in five membrane patches had a mean slope conductance of 20 ± 3 pS, with a P_K/P_{Na} of 3.2 ± 2.8. In three on-cell patch experiments with medium in the pipette, this type of channel had a unitary conductance of 27 ± 3 pS, with a mean reversal potential of −23 ± 8 mV pipette potential. In eight on-cell patches with internal solution in the pipette, the mean slope conductance was 24 ± 5 pS.

The average open time of the small potassium-selective channel measured in several on-cell patches is presented in Fig. 10*A*. The average open time of these channels varied widely, from low values of <1 ms to a value >50 ms. The membrane potential had no clear effect on the average open time.

P_o is plotted vs. membrane potential in Fig. 10*B*. The P_o values ranged from 0.005 to 0.504. This range of values is smaller than that for the large potassium-selective channels in on-cell patches (Fig. 7*C*). There was considerable variability in the observed P_o at different potentials in individual patches, in addition to great variability in these values between patches. No clear pattern relating P_o to membrane potential was apparent.

Large Nonselective Channel

This channel type was observed in only 2 of 35 on-cell patches (6%) but in 7 of 51 excised patches (14%). Examples of single-channel currents from the large, nonselective channel type are presented in Figs. 11 and 12. In Fig. 11*A*, single-channel steps at several potentials from an excised, inside-out patch in asymmetric 0.1 M NaCl and KCl are presented. The corresponding current-voltage plot is

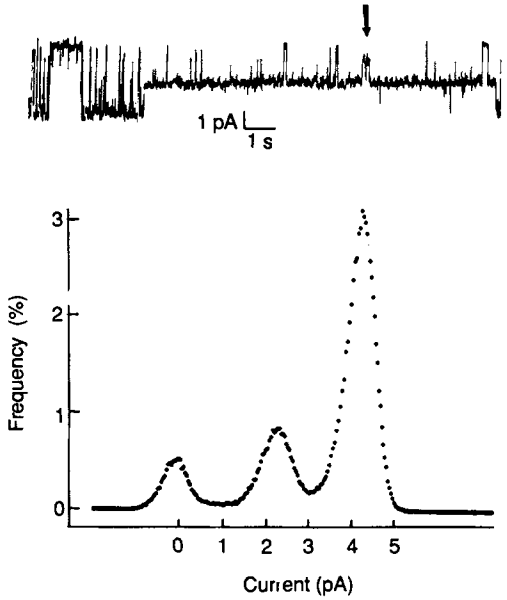

FIGURE 12. (*Top*) Rare, long-lived sojourn in the half-state, with brief transitions to the quarter-state (arrow). An excised inside-out patch bathed at both faces with 0.075 M KCl was used. The slope conductance was 206 pS. The recording bandwidth was 0–2,777 Hz; records were digitally smoothed at 200 Hz. (*Bottom*) Amplitude histogram of the record above.

presented in Fig. 11*B*. The slope conductance of the channel in this patch was 306 pS, with a reversal potential of −8.7 mV (negative pipette potential). The P_K/P_{Na} calculated from this value was 0.7.

This large-conductance channel frequently exhibited transitions to different open-channel conductance levels, as shown in Fig. 12 (top). This record is from an excised, inside-out membrane patch bathed at both membrane faces with 0.075 M KCl. We consider these different conductance levels to be subconductance states of a single channel for several reasons. First, the open-channel current in this patch never exceeded the level centered at 4.2 pA, which we term the fully open state. The vast majority of transitions were to or from the fully open state, with only a minor fraction of all transitions to or from one of the subconductance states. This would not be expected if the fully open state were due to the simultaneous opening of two or more smaller independent channels. Second, if the smaller conductance levels were due to separate channels that

opened independently of the 4.2-pA channel, there should have been instances of overlap in our records, resulting in a current level equal to the sum of the current for the large state and a smaller state. This was never observed. On the other hand, direct transitions from the fully open state to a substate and then bac' again were frequently observed. Such transitions would be a rare occurrence if the observed current level were due to the activity of separate channels.

In three excised, inside-out patches bathed in asymmetric NaCl and KCl salt solutions (two experiments were 0.1 M salt; in the third, the bath solution was 0.1 M NaCl and the pipette solution was potassium internal solution), the average slope conductance for the fully open state of these channels was 268 ± 42 pS. The average P_K/P_{Na} was 0.8 ± 0.1. This indicates poor, if any, selectivity for sodium over potassium. In one experiment where this channel type was observed in an excised, inside-out membrane patch bathed at the intracellular face with 0.5 M KCl and at the extracellular face with 0.2 M KCl, the extrapolated reversal potential was near zero, indicating poor selectivity between potassium and chloride as well.

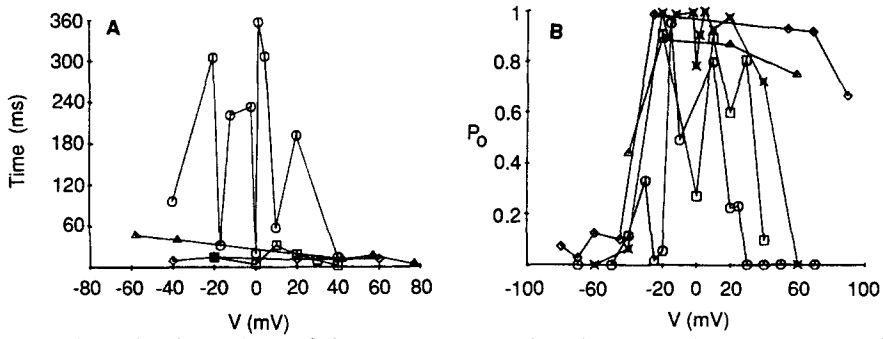

FIGURE 13. Kinetic analysis of the large nonselective channel. (*A*) Average open time plotted as a function of negative pipette potential for data from four separate excised inside-out patches. (*B*) P_o of the large nonselective channel vs. transmembrane potential for five separate excised inside-out patches. Data from individual patches are connected by lines.

In order to determine whether this channel might be affected by calcium, we varied the calcium concentration in both the bath and pipette solutions. Activity due to this channel type was observed in inside-out patches with 1.6 mM calcium at the exposed cytoplasmic membrane face. The channels were also open an appreciable fraction of the time at all five applied voltages with 0.1 mM calcium at the extracellular face and 10^{-8} M at the intracellular face. Channel activity was also observed with 10^{-8} M calcium at both membrane faces and in solutions with no added calcium.

The average open time of these channels varied from a few milliseconds to >300 ms in different patches at different potentials (Fig. 13*A*). There did not appear to be any clear dependence of average open time on membrane potential. However, when P_o was plotted as a function of membrane potential (Fig. 13*B*), a clear pattern appeared. P_o was, in general, rather high at voltages near zero membrane potential, and appeared to decline as the potential was increased or

decreased from zero. At potentials 40 mV positive and negative to zero, the channel showed occasional bursts of activity after having been inactive for several seconds. At high absolute values of potential, no openings were observed (P_o apparently became zero). The conductance and selectivity data for the four channel types have been compiled in Table I.

Channel Conductance as a Function of Ion Concentration

An ion channel can be thought of as an enzyme that catalyzes ion translocation across a membrane (Hille, 1975). In the simplest case of a channel with a single ion-binding site, the single-channel conductance near 0 mV increases as the ion concentration increases, asymptotically approaching a maximum limiting value, the G_{max} (Lauger, 1973), according to the equation

$$G = G_{max} \times [C/(C + K_m)],$$

TABLE I

Conductance and Selectivity

G, excised	G, on-cell, medium	G, on-cell, K	P_K/P_{Na}, excised
pS	*pS*	*pS*	
268±42 (3)	341 (1)	399 (1)	0.8±0.1 (3)
97±16 (11)	99±19 (5)	115±13 (5)	21.1±12 (11)
44±2 (4)	45±1 (3)	52±5 (3)	*
20±3 (5)	27±3 (3)	24±5 (8)	3.2±3 (5)

The values under the headings "G" are single-channel conductance values in picosiemens (values are represented as the mean ± standard deviation, with the number of experiments given in parentheses). "Excised" indicates experiments with asymmetric potassium and sodium solutions near a concentration of 0.1 M bathing excised, inside-out patches. "On-cell, medium" indicates experiments in which recordings were made from on-cell patches with medium in the patch-clamp pipette. "On-cell, K" indicates on-cell experiments with the pipette filled with potassium internal solution. The values listed under "P_K/P_{Na}, excised" are the potassium-over-sodium permeability ratios found from excised, inside-out patch experiments in asymmetric salt solutions. The permeability ratios for excised-patch experiments were calculated from the mean of the reversal potentials in the indicated number of experiments, using the Goldman-Hodgkin-Katz equation (Hille, 1975), and activity coefficients from Robinson and Harned (1941).

* Wide variation suggests the presence of more than one channel type. See text.

where C represents the permeant ion concentration and K_m is the concentration at which channel conductance is half-maximal. This behavior is analogous to that described in enzyme kinetics by the Michaelis-Menten equation (Hille, 1975).

We measured single-channel conductances in excised, inside-out membrane patches that were bathed on both membrane faces with identical KCl solutions at various concentrations in order to estimate the channel conductance parameters, G_{max} and K_m, under symmetric conditions. Since the current-voltage relations were linear under these conditions, the slope conductance calculated from measurements at several potentials was used to determine the channel conductance near 0 mV. As we have previously described for 0.1 M salt solutions, the single-channel currents at other KCl concentrations can be separated into four classes on the basis of conductance, though it is possible that one or more of

these classes (in particular, the medium-conductance potassium channel) may represent more than one ion channel type. In order to relate the single-channel data collected at these concentrations with the data from experiments at 0.1 M KCl, we have assumed that the largest conductance observed was that of the large, nonselective channel type, the next largest was that of the large potassium-selective channel type, and so on. We have no independent evidence supporting this assumption. However, if the single-channel data collected at various concentrations of symmetric salt solutions are separated into channel types in this way, it is possible to describe channel conductance as a function of concentration for all four types in a consistent fashion and to fit these functions with a Michaelis-Menten relation.

A plot of conductance vs. symmetric salt concentration is shown in Fig. 14. Each data point gives the mean conductance estimated from one to four membrane patches. The data for experiments in symmetric 0.5 M KCl were well

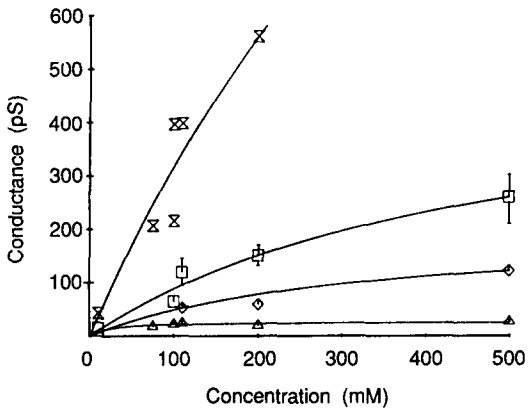

FIGURE 14. Single-channel conductance plotted as a function of symmetric cation concentration. Error bars indicate standard deviations. Data points are from excised inside-out patch experiments with symmetric KCl at the indicated concentrations, except for the points at 110 mM, which represent on-cell experiments with potassium internal solution in the pipette. Curves are least-square fittings of the data with the Michaelis-Menten equation using the best-fitting values of G_{max} and K_m given in Table II.

separated and can be associated with the three smallest channels observed at 0.2 M, since the largest conductance at 0.5 M is still smaller than the conductance of the large nonselective channel at 0.2 M KCl. We have also included in Fig. 14 (at 110 mM) data from on-cell experiments with potassium internal solution in the pipette, since the solutions across the intact cell membranes were nearly symmetric potassium salt, containing only small amounts of sodium.

In excised, inside-out patch experiments in symmetric 10 mM KCl, we observed single-channel conductances of 43, 15, and 8 pS. The 43-pS channel showed substate activity and was grouped with the large nonselective channels seen at higher concentrations. The 15-pS activity was grouped with the 100-pS potassium-selective channel. The 8-pS data point could not be assigned with certainty to either the small or the medium potassium channels and so was excluded from the plot.

We have fitted the data points in Fig. 14 with Michaelis-Menten curves by a least-squares fitting routine to estimate the maximum channel conductances and dissociation constants. The fitted curves are shown in Fig. 14, with the best-fitting values given in Table II.

DISCUSSION

This article describes some of the properties of ion channels in the exposed (apical) cell membranes of human RPE cells in tissue culture. Three of the four main channel types, and by far the largest fraction of all channels observed, are potassium selective. Thus, the apical membrane of RPE cells in culture is primarily potassium permeable, as expected from previous work on frog RPE (Miller and Steinberg, 1977). Our results are similar in this respect to Rae's (1985) finding that the lens epithelium cell membrane is dominated by potassium channels. Calcium-dependent potassium channels have been found in a variety of epithelia (Petersen and Maruyama, 1984; Rae and Levis, 1984*b*) and endothelia (Trautmann and Marty, 1984), in both apical (Garcia-Diaz et al., 1983) and basal membranes (Maruyama et al., 1983; Welsh and McCann, 1985). We could find no evidence of calcium dependence for the large nonselective channel (see p. 212), and preliminary experiments indicate none for the large potassium-selective channel as well. We also found no evidence for the presence of sodium-selective channels, although amiloride-sensitive sodium channels are found in

TABLE II

Channel Maximum Conductances and Half-Maximal Concentrations

Channel	G_{max}	K_m
	pS	*mM*
Large nonselective	2,376	646
Large potassium-selective	512	480
Medium potassium-selective	195	300
Small potassium-selective	26	22

Michaelis-Menten curves were fitted to the data points in Fig. 14 by minimizing the square of the error between the calculated and the observed conductances. The maximum channel conductances and half-maximal ion concentrations found by this fitting are listed above (see Hille, 1975). Note: medium potassium-selective data may represent more than one channel type.

many other epithelia (Benos, 1983; Jacob et al., 1985; van Driessche and Zeiske, 1985).

Some of the channel types we have recorded from human RPE cell membranes seem similar to those recorded by Rae and Levis (1984*a*, *b*) and Rae (1985) from corneal and lens epithelia. For example, these authors have reported the presence in lens epithelium of 27-, 40-, and 80, and 130-pS potassium-selective channels (Rae and Levis, 1984*b*). Two common channels recorded by Rae (1985) in corneal epithelium are potassium selective, having unitary conductances of 35 and 100 pS. The 100-pS channel has a P_K/P_{Na} of ≥ 40 and shows no dependence of gating on calcium concentration (Rae, J., personal communication).

Potassium Channels

The properties of the potassium-selective channels we observed do not resemble in detail those of the classic neuronal channels. The conductances of the two larger potassium channels at physiological ion concentrations, although larger than many other potassium channels, are somewhat smaller than that of "maxi"

potassium channels (Latorre and Miller, 1983). The calculated dissociation constants for the two larger potassium channels are much higher than those reported for sodium channels (Moczydlowski et al., 1984) and inward rectifier channels (Sakmann and Trube, 1984), although they are closer to the dissociation constants reported for acetylcholine receptor channels (Horn and Patlak, 1980) and "maxi" potassium channels (Latorre and Miller, 1983). The single-channel conductance of the smallest channel is close to the value of 27 pS reported for the inward rectifier channel of guinea pig heart (Sakmann and Trube, 1984) and the 17 pS reported for the squid potassium channel (Conti and Neher, 1980), but is larger than the 5–10 pS reported for the inward rectifier channel from tunicate (Fukushima, 1981) or rat myotube (Ohmori et al., 1981). However, the small potassium-selective channel we observe in human RPE cells is much less selective for potassium than the delayed or inward rectifier channels (Hille, 1975).

The response of these channels to changes in applied potential varied greatly from patch to patch. This variation in channel kinetics is larger than that reported for most other channels. In a typical instance, acetylcholine receptor channel open time constants ranged only from 0.24 to 0.53 ms for the fast time constant, and from 1.2 to 2.92 ms for the slow time constant in 21 patches of embryonic rat muscle (Morris et al., 1983). In contrast, the large potassium-selective channel from human RPE showed average open times ranging from 1.1 to 62 ms.

The kinetic variability that we observed was probably not due to inadvertent mixing of channel types. The evidence for this is best for the large potassium-selective channel. The measurements of channel kinetics we show were taken from the same patches as the extensive conductance and ion selectivity measurements, which formed the basis for our classification of the potassium channels. Kinetic variability was observed both in on-cell and in excised patches, as well as in patches bathed in solutions at pH 7.2 and in some early experiments in which the bath pH was more basic. Thus, the observed kinetic variability appears not to be an artifact of our experimental conditions. We believe that the large variation in open probability that we observed is the result of real variability between patches, either in the molecular properties of the channels, or in the predominance of one or another mode of channel activity in different patches (see Hess et al., 1984).

The variability in kinetic parameters that we have observed is probably not peculiar to RPE cells in tissue culture. Large variability in channel kinetics has also been observed in recordings from intact corneal and lens epithelia (Rae, 1985; Cooper et al., 1986). Furthermore, the RPE cells in our confluent cultures appeared quite similar to RPE cells in vivo, showing apical processes, basal infoldings, and Na,K-ATPase at the cell surface exposed to the culture medium (Pfeffer et al., 1986; Pfeffer, B., J. Usukura, W. O'Day, and D. Bok, manuscript in preparation). Cells in these cultures form domes, which are indicative of functional water transport (Pfeffer et al., manuscript in preparation). Physiological differentiation of apical and basal membranes can also occur in subconfluent cultures (Simons and Fuller, 1985). It is therefore likely that the electrical properties we measured from cultured cells were similar to those that would have been recorded in vivo.

Large Nonselective Channel

Large nonselective channels with conductances of 200–400 pS and several subconductance states, similar to the large-conductance channel we observed in human RPE cells, have been reported for lens and corneal epithelia from a variety of animals (Rae and Levis, 1984*a*, *b*; Rae, 1985). This channel becomes active in patches from lens tissue only after long exposure to high potentials (Rae and Levis, 1984*a*, *b*). Large nonselective channels have also been observed in recordings from isolated rods (Sather et al., 1985). Similar channels that show several substates but are anion selective have also been described in rat muscle (Blatz and Magleby, 1983), rat Schwann cells (Gray et al., 1984), apical membranes of A6 cells (Nelson et al., 1984), mouse macrophages and chicken myotubes (Schwarze and Kolb, 1984), rabbit urinary bladder epithelium (Hanrahan et al., 1985), apical membranes of MDCK cells (Kolb et al., 1985), and rat lung alveolar epithelium (Schneider et al., 1985; Krouse et al., 1986). According to Gray et al. (1984), Schwarze and Kolb (1984), and Kolb et al. (1985), these channels are approximately one-fifth as permeable to sodium as to chloride, with potassium being less permeable than sodium. The anion channels described by Nelson et al. (1984), Hanrahan et al. (1985), and Schneider et al. (1985) are also, though to a lesser extent, permeable to cations. These channels resemble, in many respects, the voltage-dependent anion channel (Schein et al., 1976) and bovine lens gap junction channel (Zampighi et al., 1985) observed in artificial membranes.

The open probability of the large nonselective channel was voltage dependent, being near 1 at potentials close to 0 mV and declining as the absolute value of the membrane potential increased. Similar voltage dependence has been reported for large-conductance anionic or nonselective channels in many tissues (Blatz and Magleby, 1983; Schwarze and Kolb, 1984; Sather et al., 1985; Nelson et al., 1984; Gray et al., 1984; Hanrahan et al., 1985; Kolb et al., 1985; Schneider et al., 1985; Krouse et al., 1986), but the voltage at which the decline in P_o begins to be most pronounced differs somewhat from preparation to preparation. Krouse et al. (1986) report that the large anion channel in rat lung alveolar epithelium begins to inactivate as the potential is changed from 0 mV. On the other hand, the large-conductance chloride channel from apical membranes of A6 cells tends to close as the potential shifts beyond +20 mV (Nelson et al., 1984), while the chloride channel from rat muscle begins to close as the potential goes beyond +30 mV (Blatz and Magleby, 1983).

The function of these large nonselective channels in pigment epithelium is not yet known. They are infrequently seen in on-cell patches, and when seen, are unlikely to be open at the normal cell resting membrane potential. This observation suggests that, despite its large unitary conductance, the large nonselective channel might not be expected to make a significant contribution to the conductance properties of RPE cells under normal conditions.

Potassium Permeability of RPE

Previous work has established that the apical RPE membrane is significantly more permeable to potassium than to sodium or chloride (Miller and Steinberg,

1977). The large potassium-selective channel, ~20 times as permeable to potassium as to sodium or chloride in excised patches, should be the most important determinant of the RPE cell membrane selectivity, since it is both the most frequently observed and the most conductive of the channels commonly found to be active in membrane patches from intact cells. The small potassium-selective channel, which is observed slightly less frequently and has one-fourth the single-channel conductance of the large potassium-selective channel, would make a lesser contribution to the membrane permeability. Its poor potassium selectivity would decrease the overall selectivity of the cell membrane. The large nonselective channel, despite its enormous unitary conductance and appreciable sodium permeability, would not be expected to increase the membrane sodium conductance appreciably, since this channel was only rarely seen to open in intact membrane patches. Weighting the permeability ratios (calculated from excised patch experiments) of each channel type by the fraction of patches that contained each channel type, we calculate the mean P_K/P_{Na} of the exposed membrane of cultured human RPE cells to be 13. This value is similar to the value for frog RPE apical membrane (Miller and Steinberg, 1977).

The present study describes the channels that underlie some of the ionic conductances previously described in intact RPE. These conductances are of fundamental importance to RPE cell physiology, since they underlie the changes in apical membrane potential and transepithelial potential produced by the decrease in the extracellular potassium concentration that follows a light flash (Schmidt and Steinberg, 1971; Steinberg et al., 1980; Oakley, 1983). These changes in potential are responsible for the generation of the retinal C-wave (Marmor and Lurie, 1979; Steinberg et al., 1985). These conductances may also be important for the role of the RPE cells in regulating the ionic environment of the photoreceptors (Miller and Steinberg, 1982; Steinberg et al., 1983; Immel and Steinberg, 1986; La Cour et al., 1986).

We thank Dean Bok for the use of tissue culture facilities, Nasser Farahbakhsh for helpful discussions, and Jeffry Lansman for help with the figures.

This work was supported by National Institutes of Health grants EY-01844 and EY-00331 to G. L. Fain, National Institutes of Health Training grant EY-07026 to J. A. Fox and B. A. Pfeffer, and by NRSA postdoctoral fellowship EY-5825 and a grant from the National Society to Prevent Blindness to J. A. Fox. Human tissue was obtained through the Jules Stein Eye Institute Eye Bank.

Original version received 4 May 1987 and accepted version received 21 September 1987.

REFERENCES

Benham, C. D., and T. B. Bolton. 1983. Patch-clamp studies of slow potential-sensitive potassium channels in longitudinal smooth muscle of rabbit jejunum. *Journal of Physiology.* 340:469–486.

Benos, D. J. 1983. Ionic channels in epithelia. *Comments in Molecular and Cellular Biophysics.* 2:111–128.

Blatz, A. L., and K. L. Magleby. 1983. Single voltage-dependent chloride-selective channels of large conductance in cultured rat muscle. *Biophysical Journal.* 43:237–241.

Colquhoun, D., and F. J. Sigworth. 1983. Fitting and statistical analysis of single-channel

records. *In* Single-Channel Recording. B. Sakmann and E. Neher, editors. Plenum Publishing Corp., New York. 191–263.

Conti, F., and E. Neher. 1980. Single channel recordings of K^+ currents in squid axons. *Nature.* 285:140–143.

Cooper, K., J. Tang, J. Rae, and R. Eisenberg. 1986. A cation channel in frog lens epithelia responsive to pressure and calcium. *Journal of Membrane Biology.* 93:259–269.

Crawford, B. J. 1983. Some factors controlling cell polarity in chick retinal pigment epithelial cells in clonal culture. *Tissue & Cell.* 15:993–1005.

Fenwick, E., A. Marty, and E. Neher. 1982. Sodium and calcium channels in bovine chromaffin cells. *Journal of Physiology.* 331:599–635.

Fernandez, J. M., A. P. Fox, and S. Krasne. 1984. Membrane patches and whole-cell membranes: a comparison of electrical properties in rat clonal pituitary (GH3) cells. *Journal of Physiology.* 356:565–585.

Fox, J. A. 1985. Improved method for illuminating patch-clamp pipettes for fire-polishing. *Journal of Neuroscience Methods.* 15:239–241.

Fox, J. A., B. A. Pfeffer, and G. L. Fain. 1985. Patch-clamp studies on human retinal pigment epithelium. *Investigative Ophthalmology and Visual Science.* 26(Suppl.):117. (Abstr.)

Fox, J. A., B. A. Pfeffer, and G. L. Fain. 1986. Potassium channels in human retinal pigment epithelium. *Biophysical Journal.* 49:217*a*. (Abstr.)

Fox, J. A., B. A. Pfeffer, G. L. Fain, and D. Bok. 1984. Ion channels in human retinal pigment epithelium. *Society for Neuroscience Abstracts.* 10(Pt.2):870.

Fukushima, Y. 1981. Single channel potassium currents of the anomalous rectifier. *Nature.* 294:368–371.

Garcia-Diaz, J. F., W. Nagel, and A. Essig. 1983. Voltage dependent K conductance at the apical membrane of *Necturus* gallbladder. *Biophysical Journal.* 43:269–278.

Gray, P. T. A., S. Bevan, and J. M. Ritchie. 1984. High conductance anion-selective channels in rat cultured Schwann cells. *Proceedings of the Royal Society of London, Series B.* 221:395–409.

Griff, E. R., and R. H. Steinberg. 1982. Origin of the light peak: in vitro study of *Gekko gekko.* *Journal of Physiology.* 331:637–652.

Hamill, O. P., A. Marty, E. Neher, B. Sakmann, and F. J. Sigworth. 1981. Improved patch-clamp techniques for high-resolution current recording from cells and cell-free patches. *Pflügers Archiv.* 391:85–100.

Hanrahan, J. W., W. P. Alles, and S. A. Lewis. 1985. Single anion-selective channels in basolateral membrane of a mammalian tight epithelium. *Proceedings of the National Academy of Sciences.* 82:7791–7795.

Hess, P., J. B. Lansman, and R. W. Tsien. 1984. Different modes of Ca channel gating behaviour favoured by dihydropyridine Ca antagonists. *Nature.* 311:538–544.

Hille, B. 1975. Ionic selectivity of Na and K channels of nerve membranes. *In* Membranes: a Series of Advances. G. Eisenman, editor. Marcel Dekker, New York. 3:255–323.

Horn, R., and J. Patlak. 1980. Single channel currents from excised patches of muscle membrane. *Proceedings of the National Academy of Sciences.* 77:6930–6934.

Horn, R., C. Vandenburg, and K. Lange. 1984. Statistical analysis of single sodium channels. Effects of *N*-bromoacetamide. *Biophysical Journal.* 45:323–335.

Immel, J., and R. H. Steinberg. 1986. Spatial buffering of K^+ by the retinal pigment epithelium in frog. *Journal of Neuroscience.* 6:3197–3204.

Jacob, T. J. C., J. A. Bangham, and G. Duncan. 1985. Characterization of a cation channel on the apical surface of the frog lens epithelium. *Quarterly Journal of Experimental Physiology.* 70:403–421.

Kolb, H.-A., C. D. A. Brown, and H. Murer. 1985. Identification of a voltage-dependent anion channel in the apical membrane of a Cl-secretory epithelium (MDCK). *Pflügers Archiv.* 403:262–265.

Krouse, M. E., G. T. Schneider, and P. W. Gage. 1986. A large anion selective channel has seven conductance levels. *Nature.* 319:58–60.

Labarca, P., J. Lindstrom, and M. Montal. 1984. Acetylcholine receptor in planar lipid bilayers. *Journal of General Physiology.* 83:473–496.

La Cour, M., H. Lund-Andersen, and T. Zeuthen. 1986. Potassium transport of the frog retinal pigment: autoregulation of potassium activity in the subretinal space. *Journal of Physiology.* 375:461–479.

Lasansky, A., and F. W. De Fisch. 1966. Potential, current, and ionic fluxes across the isolated retinal pigment epithelium and choroid. *Journal of General Physiology.* 49:913–924.

Latorre, R., and C. Miller. 1983. Conduction and selectivity in potassium channels. *Journal of Membrane Biology.* 71:11–30.

Lauger, P. 1973. Ion transport through pores: a rate-theory analysis. *Biochimica et Biophysica Acta.* 311:423–441.

Lindemann, B. 1984. Fluctuation analysis of sodium channels in epithelia. *Annual Review of Physiology.* 46:497–515.

Linsenmeier, R. A., and R. H. Steinberg. 1982. Origin and sensitivity of the light peak in the intact cat eye. *Journal of Physiology.* 331:653–673.

Linsenmeier, R. A., and R. H. Steinberg. 1983. A light-evoked interaction of the apical and basal membranes of the retinal pigment epithelium: the c-wave and the light peak. *Journal of Neurophysiology.* 50:136–147.

Marmor, M. F., and M. Lurie. 1979. Light-induced electrical responses of the retinal pigment epithelium. *In* The Retinal Pigment Epithelium. K. Zinn and M. F. Marmor, editors. Harvard University Press, Cambridge, MA. 226–244.

Marty, A., and E. Neher. 1983. Tight-seal whole-cell recording. *In* Single-Channel Recording. B. Sakmann and E. Neher, editors. Plenum Publishing Corp., New York. 107–122.

Maruyama, Y., D. V. Gallacher, and O. H. Petersen. 1983. Voltage and Ca^{2+}-activated K^+ channel in baso-lateral acinar cell membranes of mammalian salivary glands. *Nature.* 302:827–829.

Mejia, R., and C. Chang. 1970. Time series analysis: theory and practice. Technical Report Number 4. National Institutes of Health, U.S. Department of Health, Education and Welfare, Bethesda, MD. II-1–II-6.

Miller, S. S., and R. H. Steinberg. 1977. Passive ionic properties of frog retinal pigment epithelium. *Journal of Membrane Biology.* 36:337–372.

Miller, S. S., and R. H. Steinberg. 1982. Potassium transport across the frog retinal pigment epithelium. *Journal of Membrane Biology.* 67:199–209.

Moczydlowski, E., S. Garber, and C. Miller. 1984. Batrachotoxin-activated Na^+ channels in planar lipid bilayers. *Journal of General Physiology.* 84:665–686.

Morris, C. E., B. S. Wong, M. B. Jackson, and H. Lecar. 1983. Single-channel currents activated by curare in cultured embryonic rat muscle. *Journal of Neuroscience.* 3:2525–2531.

Nelder, J. A., and R. Mead. 1965. A simplex method for function minimization. *The Computer Journal.* 7:308–313.

Nelson, D. J., J. M. Tang, and L. G. Palmer. 1984. Single-channel recordings of apical membrane chloride conductance in A6 epithelial cells. *Journal of Membrane Biology.* 80:81–89.

Oakley, B. 1977. Potassium and the photoreceptor-dependent pigment epithelial hyperpolarization. *Journal of General Physiology.* 70:405–425.

Oakley, B. 1983. Effects of maintained illumination upon $[K^+]_o$ in the subretinal space of the isolated retina of the toad. *Vision Research.* 23:1325–1337.

Oakley, B., S. S. Miller, and R. H. Steinberg. 1978. Effects of intracellular potassium upon the electrogenic pump of frog retinal pigment epithelium. *Journal of Membrane Biology.* 44:281–307.

Ohmori, H., S. Yoshida, and S. Hagiwara. 1981. Single K^+ channel currents of anomalous rectification in cultured rat myotubes. *Proceedings of the National Academy of Sciences.* 78:4960–4964.

Patlak, J. B., and R. Horn. 1982. Effect of *N*-bromoacetamide on single sodium channel currents in excised membrane patches. *Journal of General Physiology.* 79:333–351.

Petersen, O. H., and Y. Maruyama. 1984. Calcium-activated potassium channels and their role in secretion. *Nature.* 307:693–696.

Pfeffer, B. A., V. A. Clark, J. G. Flannery, and D. Bok. 1986. Membrane receptors for retinol-binding protein in cultured human retinal pigment epithelium. *Investigative Ophthalmology and Visual Science.* 27:1031–1040.

Rae, J. L. 1985. The application of patch clamp to ocular epithelia. *Current Eye Research.* 4:409–420.

Rae, J. L., and R. A. Levis. 1984*a*. Patch clamp recordings from the epithelium of the lens obtained using glasses selected for low noise and improved sealing properties. *Biophysical Journal.* 45:144–146.

Rae, J., and R. A. Levis. 1948*b*. Patch voltage clamp of lens epithelial cells: theory and practice. *Molecular Physiology.* 6:115–162.

Robinson, R. A., and H. S. Harned. 1941. Some aspects of the thermodynamics of strong electrolytes from electromotive force and vapor pressure measurements. *Chemical Reviews.* 28:419–477.

Sakmann, B., and G. Trube. 1984. Conductance properties of single inwardly rectifying potassium channels in ventricular cells from guinea-pig heart. *Journal of Physiology.* 347:641–657.

Sather, W. A., R. D. Bodoia, and P. B. Detwiler. 1985. Does the plasma membrane of the rod outer segment contain more than one type of ion channel? *Neuroscience Research.* 2(Suppl.):S89–S99.

Schein, S. J., M. Colombini, and A. Finkelstein. 1976. Reconstitution in planar lipid bilayers of a voltage-dependent anion-selective channel obtained from paramecium mitochondria. *Journal of Membrane Biology.* 30:99–120.

Schmidt, R., and R. H. Steinberg. 1971. Rod-dependent intracellular responses to light recorded from the pigment epithelium of the cat retina. *Journal of Physiology.* 317:71–91.

Schneider, G. T., D. I. Cook, P. W. Gage, and J. A. Young. 1985. Voltage sensitive, high-conductance chloride channels in the luminal membrane of cultured pulmonary alveolar (type II) cells. *Pflügers Archiv.* 404:354–357.

Schwarze, W., and H.-A. Kolb. 1984. Voltage-dependent kinetics of an anionic channel of large unit conductance in macrophages and myotube membranes. *Pflügers Archiv.* 402:281–291.

Simons, K., and S. Fuller. 1985. Cell surface polarity in epithelia. *Annual Review of Cell Biology.* 1:243–288.

Steinberg, R. H., R. A. Linsenmeier, and E. R. Griff. 1983. Three light-evoked responses of the retinal pigment epithelium. *Vision Research.* 23:1315–1323.

Steinberg, R. H., R. A. Linsenmeier, and E. R. Griff. 1985. Retinal pigment epithelial cell contributions to the electroretinogram and electrooculogram. *Progress in Retinal Research.* 4:33–66.

Steinberg, R. H., and S. S. Miller. 1979. Transport and membrane properties of the retinal pigment epithelium. *In* The Retinal Pigment Epithelium. K. Zinn and M. F. Marmor, editors. Harvard University Press, Cambridge, MA. 205–225.

Steinberg, R. H., B. Oakley, and G. Niemeyer. 1980. Light-evoked changes in $[K^+]_o$ in retina of intact cat eye. *Journal of Neurophysiology.* 44:897–921.

Taub, M. 1984. Viruses in the study of the polarity of epithelial membranes. *In* Tissue Culture of Epithelial Cells. M. Taub, editor. Plenum Publishing Corp., New York, NY. 127–144.

Trautmann, A., and A. Marty. 1984. Activation of Ca-dependent K channels by carbamoylcholine in rat lacrimal glands. *Proceedings of the National Academy of Sciences.* 81:611–615.

Tsuboi, S., R. Manabe, and S. Iizuka. 1986. Aspects of electrolyte transport across isolated dog retinal pigment epithelium. *American Journal of Physiology.* 250:F781–F784.

van Driessche, W., and W. Zeiske. 1985. Ionic channels in epithelial cell membranes. *Physiological Reviews.* 65:833–903.

Welsh, M. J., and J. D. McCann. 1985. Intracellular calcium regulates basolateral potassium channels in a chloride-secreting epithelium. *Proceedings of the National Academy of Sciences.* 82:8823–8826.

Zampighi, G. A., J. E. Hall, and M. Kreman. 1985. Purified lens junctional protein forms channels in planar lipid films. *Proceedings of the National Academy of Sciences.* 82:8468–8472.